

Supplementary Information for

The purine biosynthesis regulator PurR moonlights as a virulence regulator in *Staphylococcus aureus*

William E. Sause, Divya Balasubramanian, Irnov Irnov, Richard Copin, Mitchell J. Sullivan, Alexis Sommerfield, Rita Chan, Avantika Dhabaria, Manor Askenazi, Beatrix Ueberheide, Bo Shopsin, Harm van Bakel, and Victor J. Torres

Corresponding Author: Victor J. Torres
E-mail: Victor.Torres@nyulangone.org

This PDF file includes:

Supplementary text
Figs. S1 to S3
Captions for datasets S1 to S3
Tables S1 to S2
References for SI reference citations

Other supplementary materials for this manuscript include the following:

Datasets S1 to S3

Supplementary Text

Supplementary Materials and Methods

Bacterial strains. *S. aureus* strain JE2 is a plasmid-cured derivative of USA300 LAC and serves as the host strain for all mutants within the Nebraska Transposon Mutant Library (NTML) (1). *S. aureus* strain AH-LAC (2) is also a plasmid cured derivative of USA300 LAC and was used in addition to JE2 due to antibiotic resistance cassette compatibility in the case of the *purR::bursa/ΔΔΔΔ* mutant. The $\Delta purR$ isogenic mutant was generated using the *pIMAY* allelic exchange plasmid by replacing the *purR* locus with the *aphA-3* gene encoding kanamycin resistance (3). To complement the *purR* mutant, the *purR* locus was cloned into *pOS1-plgt* and the resulting construct, *pOS1-plgt-purR*, transformed into the $\Delta purR::kan$ mutant. For chromosomal complementation, the *purR* locus, which lies in an operon with the upstream gene *ipk*, was cloned with *ipk* and its promoter into the *pJC1036* complementation plasmid (4). Then, using inverse PCR (iPCR), the *ipk* gene and a 13 base pair intergenic region between *purR* and *ipk* were removed, creating a fusion between *purR* and the promoter upstream of *ipk*. To generate the complemented strains, we transformed *pJC1306-purR* or *pJC1306* (empty vector) plasmids into RN4220 carrying pRN7023, which contains an integrase and thus allows integration of pJC1306 into the SaPI1 site. The SapI1 locus from RN4220 was then transduced with phage $\Phi 80$ into the $\Delta purR::kan$ mutant. Phage lysates generated from Nebraska Transposon Mutant Library (NTML) mutants obtained from BEI Resources or our library were transduced with phage $\Phi 80$ into recipient strains. For a complete list of strains and primers, please see SI Appendix, Tables S1 and S2 respectively.

Growth Curves. *S. aureus* strains grown overnight in TSB were diluted 1/100,000 in either TSB or Roswell Park Memorial Institute medium (RPMI 1640; Invitrogen) supplemented with 1% Casamino Acids (RPMI+CAS). Diluted cultures were then grown at 37°C for 24 hours in 100-well Honeycomb plates (Bioscreen) using an automated growth curve analysis system (Bioscreen C). OD₆₀₀ measurements were recorded every 30 min.

Exoprotein analysis. Proteins were concentrated from 3-h culture supernatants using 10% (vol/vol) trichloroacetic acid (TCA) precipitation as described previously (5). Protein visualization was achieved by separating samples using SDS-12% PAGE and staining with SYPRO Ruby (Invitrogen). To assess the production of specific products, proteins were resolved with 12% SDS-PAGE, transferred to a nitrocellulose membrane, and then probed with the indicated primary antibody. Alexa Fluor 680–anti-rabbit antibody was used as a secondary antibody, and the membranes were visualized using the Odyssey infrared imaging system (Li-Cor Biosciences, Lincoln, NE).

RNA isolation. RNA isolation and sample preparation for RNA-Seq was performed as previously outlined by Carroll *et al* (6). Briefly, overnight cultures of USA300 wild-type and the isogenic $\Delta purR$ were diluted 1:100 and replicas for each strain grown to exponential phase (3 hr) or stationary phase (5 hr) in TSB at 37°C while shaking at 180 RPM. Cells were spun down, supernatants removed, and pellets frozen at -80°C overnight. Pellets were thawed and resuspended in TE buffer (pH=8.0). Resuspended cells were transferred to a Lysing Matrix B tube (MP Biomedicals) and disrupted in a FastPrep-24 homogenizer (MP Biomedicals) for 60 sec at 4.5 M/s. Samples were then centrifuged for 1 min and the RNA isolated using RNeasey (Qiagen) mini spin columns. Purified RNA was treated with DNase I (Ambion) and cleaned up according to manufacturer's instructions. RNA quality was assessed on a formamide gel.

Transcriptome sequencing (RNA-Seq) libraries were generated using an Illumina TruSeq Stranded Total RNA Library Prep kit, after ribodepletion was performed with an Epicenter Ribo-Zero Gold kit (catalog no. RZE1224), starting from 2 µg of DNase I-treated total RNA, following the manufacturer's protocol, with the exception that 13 cycles of PCR were performed to amplify the libraries, to keep the duplication rate lower than that which occurs with the recommended 15 cycles. The amplified libraries were purified using AMPure beads, quantified by

Qubit and qPCR, and visualized in an Agilent Bioanalyzer. The libraries were pooled equimolarly and loaded on an Illumina MiSeq flow cell (9v2) and run as paired 150-nucleotide reads.

Differential gene expression analysis. Raw reads were first trimmed by removing Illumina adapter sequences from 3' ends using cutadapt (7), and by removing 3' read sequences if more than 20 bases with $Q \geq 20$ were present. Paired-end reads were then mapped to the FPR3757 (NC_007793) reference genome using Bowtie2 (8), and htseq-count (9) was used to produce strand-specific transcript count summaries. Raw fragment (i.e., paired-end read) counts were then combined into a numeric matrix, with genes in rows and samples in columns, and used as input for differential gene expression analysis with the limma R package (10) in Bioconductor. Normalization factors were computed on the data matrix using the weighted trimmed mean of M-values (TMM) method, followed by voom (11) mean-variance transformation in preparation for Limma linear modeling. Only genes with expression levels ≥ 1 FPKM (fragments per kb per million reads) in at least 50% of samples, and a length ≥ 200 bp, were retained for further analysis. Filtered data were fitted to a design matrix containing all sample groups, and pairwise comparisons were performed between the groups of interest. Finally, eBayes adjusted P-values were corrected for multiple testing using the Holm method and used to select genes with significant expression differences ($q \leq 0.05$).

Quantitative real time polymerase chain reaction (qRT-PCR). qRT-PCR experiments were conducted as described previously (12). Briefly, RNA from exponentially grown USA300 was purified as described above and used to perform qRT-PCR in a one-step reaction using Reverse Transcriptase Mastermix (QuantiTect) and SYBR green master mix (Qiagen) in a QuantStudio 3 Real-Time PCR system (Applied Biosystems). Target genes in each strain were compared to the corresponding gene in wild-type cells.

Gene ontology enrichment analyses. Gene ontology (GO) biological process (BP) enrichment analyses were performed using the gProfileR R v0.6.4 package (13). GO terms were assigned to all genes in the FPR3757 reference genome using InterProScan 5.15-54.0 (14). The background gene set was restricted to the filtered gene matrix used for differential expression analysis. An ordered query was used, ranking genes by log 2-fold-change for differential gene expression analyses. P values were corrected using the g:SCS algorithm to account for multiple comparisons.

Sample preparation and data analysis for quantitative mass spectrometry.

Overnight cultures of wild-type JE2 or $\Delta purR$ were diluted 1:100 into 20 mL of TSB (in 50 mL Falcon tube) and grown at 37 °C with shaking (180 rpm) for 3 hr. To analyze the exoproteomes, culture supernatants were filtered and TCA precipitated as described above. The protein isolates were reduced, alkylated, trypsin digested, desalted and loaded onto an EASY spray column as described in Becker *et al* (15). The peptides were eluted using a 70 min gradient into an Orbitrap Q Exactive HF-X Mass Spectrometer (Thermo Fisher Scientific). The top 20 ions per full scan were fragmented and put on a dynamic exclusion list for 30 seconds.

To analyze the intracellular proteomes, cells from 3-hr cultures were transferred onto a 0.45 μ m nylon membrane (Millipore) by vacuum filtration and quickly washed with 5 mL cold PBS. The membrane filters were then dropped into petri dishes containing 1.5 mL cold lysis buffer (10 mM Tris-HCl pH 8.0, 8M Urea, 1x Halt protease inhibitor (Thermo Fisher)). Cells were then washed off the membrane filters and subjected to mechanical lysis using 0.1 mm glass beads in a FastPrep-24 homogenizer (MP Biomedicals) for 3 x 30 sec at 6 M/s. To improve the recovery of membrane proteins, sodium deoxycholate was added to the lysates at a final concentration of 0.15% and the mixtures were incubated on ice for 30 min. The samples were clarified by centrifugation at 13,000 x g for 15

min and the supernatants were digested and analyzed by liquid chromatography-mass spectrometry (LC-MS) analysis as described above.

The raw files were searched using SEQUEST (16) within Proteome discoverer (version 1.4) against the UniProt USA300 protein database. The mass tolerance was set to 10 ppm for the parent and 0.02 Da for the fragment masses. Trypsin-specific cleavage was selected with 2 missed cleavages. Carbamidomethylation of Cys was set as a static modification. Oxidation of Met, deamidation of Asn and Gln, and acetylation of the protein N terminus were set as variable modifications. Peptides were filtered to better than 1% FDR using a target-decoy database strategy and proteins require at least two unique peptides to be reported. Statistical differences in protein fold changes were determined using *t*-tests. The complete dataset with associated *p*-values and False Discovery Rate estimates is provided in the Supplementary Table 1.

Cytotoxicity Assays. Primary human neutrophils were intoxicated as described previously. Briefly, *S. aureus* overnight cultures were sub-cultured for 3 hours to exponential phase and their supernatants retained and filter sterilized. Supernatants were diluted 2-fold in a 96-well plate (20 to 2.5%). PMNs were isolated as described by Reyes-Robles *et al.* (17) and normalized to 200,000 cells per 80 μ l RPMI supplemented with 10% fetal bovine serum (FBS). PMNs (80 μ l) were then pipetted into each well, and the supernatant-PMN mixtures incubated in a 37°C-5% CO₂ incubator for 1 h. To assess toxicity, 10 μ l of CellTiter 96 Aqueous One solution (CellTiter; Promega) was added to the 96-well plate, and the mixture was incubated at 37°C in 5% CO₂ for 1.5 h. PMN viability was assessed with a PerkinElmer EnVision 2103 multilabel reader at an absorbance of 492 nm.

Murine Sepsis Model. Exponentially grown *S. aureus* were washed, resuspended in 1X phosphate-buffered saline, measured for cell density (optical density at 600 nm [OD₆₀₀]), normalized, and then plated for CFU. All mouse

infections, including CFU and lethality experiments, were conducted with inoculums of 2.5×10^7 CFU. Retro-orbital infections (100- μ l inoculum) were performed on 5-week-old female ND4 Swiss-Webster mice (Envigo) that had been anesthetized intraperitoneally with 300 μ l of Avertin (2,2,2-tribromoethanol dissolved in tert-amyl alcohol and diluted to a final concentration of 2.5% [vol/vol] in sterile saline). To examine for tissue colonization at either 4 or 20 h post-infection, the mice were euthanized with CO₂, and the indicated organs were harvested as described previously (18). For acute/survival experiments, mice administered retro-orbital infections were monitored every 4 to 6 h for signs of morbidity (hunched posture, lack of movement, paralysis, and inability to acquire food or water), at which time the animals were euthanized and survival curves were plotted.

Figures

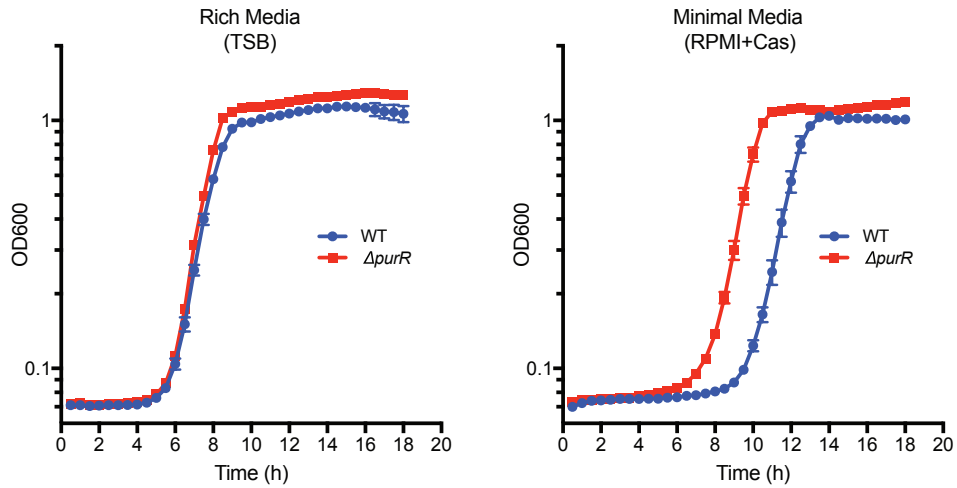


Fig. S1. Growth curve comparisons between wild-type USA300 and the isogenic *purR* mutant demonstrate that the two strains grow with similar kinetics in rich media (TSB) but that the *purR* mutant has growth advantage in minimal media (RPMI).

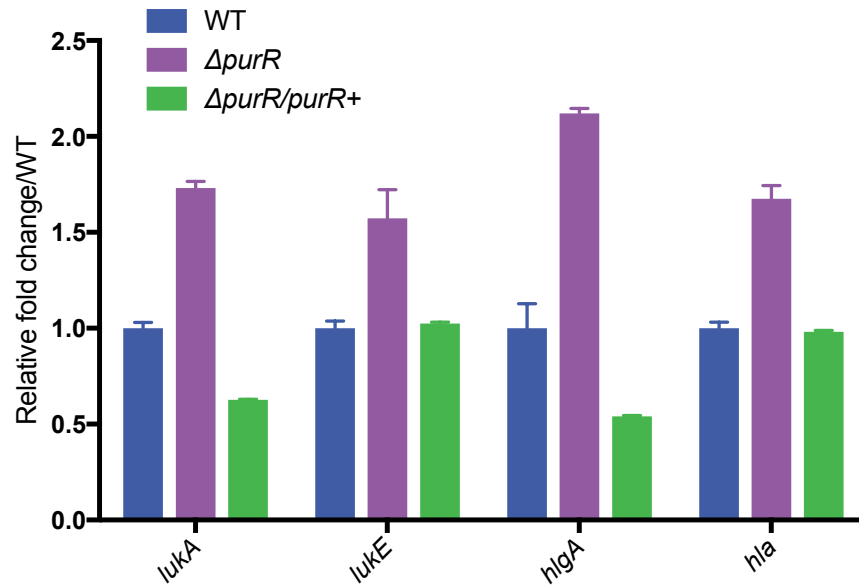


Fig. S2. qRT-PCR performed on RNA isolated from exponentially grown USA300 demonstrates that the *purR* mutant displays elevated transcript levels for toxin-encoding genes when compared to wild-type or the complemented *purR* mutant. Transcript levels were assessed from two independent colonies and fold-changes were calculated relative to wild-type expression levels.

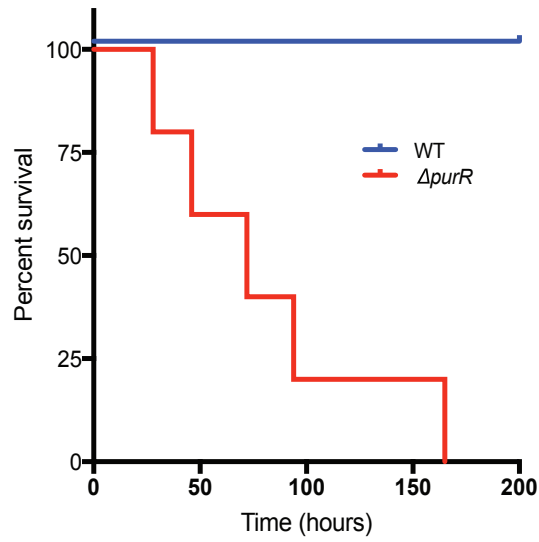


Fig. S3. In an intravenous infection (2.5×10^7 CFU) using bacteria grown to stationary phase (5 hr), the isogenic *purR* mutant is still acutely lethal to mice compared to wild-type USA300 (n = 5 mice/strain).

Datasets and Tables

Dataset S1 (separate file). Complete dataset showing peptide-to-spectrum matches (PSMs) and fold-changes in both endoprotein and exoprotein levels in the *purR* mutant compared to wild-type *S. aureus*. Includes *p*-values and False Discovery Rate estimates.

Dataset S2 (separate file). Complete RNASeq dataset for wild-type *S. aureus* and the *purR* mutant at both exponential and stationary growth phases.

Dataset S3 (separate file). PurR boxes identified using FIMO (Find Individual Motif Occurrences) version 5.0.1. Also included are the putative direct PurR target genes based on the presence of a PurR box in the 1-kb upstream region and significant increased gene expression in the *purR* mutant vs. wild-type *S. aureus* at 3 or 5 hours growth.

Table S1. Strains used in this study.

VJT#	Strain Name	Description	Reference
31.81	JE2 WT	Erm ^S USA300 parent strain	(1)
15.77	AH LAC WT	Erm ^S USA300 parent strain	(2)
60.89	BL21 <i>pET41b-purR</i>	<i>E. coli</i> BL21 carrying the plasmid <i>pET41b-purR</i>	This study
63.100	JE2 <i>ccpA::bursa</i>	JE2 carrying the <i>bursa aurealis</i> transposon in the <i>ccpA</i> gene	(1)
63.94	JE2 <i>malR::bursa</i>	JE2 carrying the <i>bursa aurealis</i> transposon in the <i>malR</i> gene	(1)
63.95	JE2 <i>purR::bursa</i>	JE2 carrying the <i>bursa aurealis</i> transposon in the <i>purR</i> gene	(1)
62.59	JE2 <i>rbsR::bursa</i>	JE2 carrying the <i>bursa aurealis</i> transposon in the <i>rbsR</i> gene	(1)
62.60	JE2 <i>scrR::bursa</i>	JE2 carrying the <i>bursa aurealis</i> transposon in the <i>scrR</i> gene	(1)
49.77	JE2 Δ <i>purR::kan</i>	JE2 carrying the <i>aphA3</i> cassette in the <i>purR</i> gene	This study
50.36	JE2 WT	JE2 WT carrying <i>pOS1-plgT</i>	This study
50.38	JE2 Δ <i>purR::kan/purR+</i>	JE2 Δ <i>purR::kan</i> carrying <i>pOS1-plgT-purR</i>	This study
50.39	JE2 Δ <i>purR::kan</i>	JE2 Δ <i>purR::kan</i> carrying <i>pOS1-plgT</i>	This study
56.53	JE2 WT	JE2 WT carrying <i>pJC1306</i> empty vector in the <i>SapI</i> site	(12)

56.54	JE2 Δ purR::kan	JE2 Δ purR::kan carrying pJC1306 empty vector in the SapI site	This study
59.47	JE2 Δ purR::kan/purR+	JE2 Δ purR::kan carrying pJC1306 expressing Pipk-purR in the SapI site	This study
62.26	JE2 purA::bursa	JE2 carrying pJC1306 empty vector transduced with the bursa aurealis transposon in the purA gene	This study
62.61	JE2 purF::bursa	JE2 carrying the bursa aurealis transposon in the purF gene	(1)
62.27	JE2 purH::bursa	JE2 carrying pJC1306 empty vector transduced with the bursa aurealis transposon in the purH gene	This study
62.26	JE2 Δ purR::kan/ purA::bursa	JE2 Δ purR::kan carrying pJC1306 empty vector transduced with the bursa aurealis transposon in the purA gene	This study
63.63	JE2 Δ purR::kan/ purF::bursa	JE2 Δ purR::kan carrying the bursa aurealis transposon in the purF gene	This study
62.28	JE2 Δ purR::kan/ purH::bursa	JE2 Δ purR::kan carrying pJC1306 empty vector transduced with the bursa aurealis transposon in the purH gene	This study
47.15	AH LAC $\Delta\Delta\Delta\Delta$	AH LAC carrying Δ lukAB hlgACB::tet lukED::kan PVL::spec	(19)
62.63	AH LAC purR::bursa/ $\Delta\Delta\Delta\Delta$	AH LAC Δ lukAB hlgACB::tet lukED::kan PVL::spec carrying the bursa aurealis transposon in the purR gene	This study
53.93	JE2 hla::bursa	JE2 carrying the bursa aurealis transposon in the hla gene	(1)
63.88	JE2 Δ purR::kan/ hla::bursa	JE2 Δ purR::kan carrying the bursa aurealis transposon in the hla gene	This study
63.55	JE2 SAUSA300_0408::bursa	JE2 carrying the bursa aurealis transposon in the SAUSA300_0408 gene	(1)
65.98	JE2 Δ purR::kan/ SAUSA300_0408::bursa	JE2 Δ purR::kan carrying the bursa aurealis transposon in the SAUSA300_0408 gene	This study
66.54	JE2 fnbA::bursa	JE2 carrying the bursa aurealis transposon in the fnbA gene	(1)
65.97	JE2 Δ purR::kan/ fnbA::bursa	JE2 Δ purR::kan carrying the bursa aurealis transposon in the fnbA gene	This study

Table S2. Primers used in this study.

Primers	
F.purR.up	CAAGTAAATACTAAGTAATTAGATGGAGAAAATTAC
R.purR.up.kan	gtacCtagattTagATgtctaAaaag CATAAAAACAATTCTCTCGCTTCGTTTA
F.purR.down.kan	GTtcgctggggttAtcgtcgag GtattTaatggAagAaaaattagAtgctgt
R.purR.down	TCGCGGAATTCACCATCTGG
F.PIMAY.FAST	GGTACCCAGCTTTTGTTCCTTTAGTGAGG
R.PIMAY.FAST	GAGCTCCAATTCGCCCTATAGTGAGTCG
F.purR.PIMAYFAST	CGACTCACTATAGGGCGAATTGGAGCTCCAAGTAA ATACTAAGTAATTAGATGGAGAAAATTAC
R.purR.PIMAYFAST	CCTCACTAAAGGGAACAAAAGCTGGGTACC TTCTTACTTCAAAAATACGAGCATCATTC
F.plgT purR.Ndel	cccccc cataTg ggAtagaagGgTtgAAAaGAtGaGAtA
R.plgT purR.BamHI	cccccc ggatcc ATACTAAAACCTTTTTATGAAAACCTTAGATAAAC
F.intergenic_ipk_pJC1306	CCCCCC CTGCAG ATAAGACATATAGAGATGTT
R.purR_rev_pJC1306	CCCCCC GGATCC TTATGAAAACCTTAGATAAAC
F.iPCR_purR_ATG	ATGAGATATAAACGAAGCGA
R.iPCR_ipk	TTTCCGCCCTCTTTTCGTTA
F.purR_pET41b	CCCCCCCATATGAGATATAAACGAAGCGAGAG
R.purR_pET41b	CCCCCCCTCGAGTGAAAACCTTAGATAAACTGT
Promoter Binding Primers	
purA For	AAAAGTTTTTCCGTACAATA
purA Rev (biotin)	ACATGTGAGCACCTCCAAGT
phoB For	TTTTCCACCTCAAATTATAT
phoB Rev (biotin)	TAAGACATCCTCCTGAGTAT
sarA For	GTCTATACGTTATTCCGATT
sarA Rev (biotin)	AAATTAACCTTTTAGCTTATC
fnbA For (biotin)	CTAAGATTGTTTTTCACTAT
fnbA Rev	GTATAAAAAATACAAGCCTT
ssl11 For	CTTTGATAAATACATAGATT
ssl11 Rev (biotin)	AATTCTATGCTCCCAATTTT
qRT-PCR Primers	
lukA qRT-PCR	TTCCCAATATCATCCGGTGCTG
lukA qRT-PCR	GTTATCAGCAGCAACGACTCAAGC
lukE qRT-PCR	GAAATGGGGCGTTACTCAA
lukE qRT-PCR	GAATGGCCAAATCATTTCGTT

<i>hlgA</i> qRT-PCR	AATCGGAGGCAGTGGCTCATTCAA
<i>hlgA</i> qRT-PCR	GGACCAGTTGGGTCTTGTGCAAAT
<i>S-PV</i> qRT-PCR	CCAATAAATTCTGGATTGAAGTTACCT
<i>S-PV</i> qRT-PCR	GCTCAAGACAAAGCAACTTAAATGC
hla P1-RT	AAAAAACTGCTAGTTATTAGAACGAAAGG
hla P2-RT	GGCCAGGCTAAACCACTTTTG
16s rRNA	CGGTTTCGCTGCCCTTTGTATTGT
16s rRNA	TGAGATGTTGGGTTAAGTCCCGCA

References

1. Fey PD, *et al.* (2013) A genetic resource for rapid and comprehensive phenotype screening of nonessential *Staphylococcus aureus* genes. *Mbio* 4(1):e00537-00512.
2. Boles BR, Thoendel M, Roth AJ, & Horswill AR (2010) Identification of genes involved in polysaccharide-independent *Staphylococcus aureus* biofilm formation. *PloS one* 5(4):e10146.
3. Monk IR, Shah IM, Xu M, Tan MW, & Foster TJ (2012) Transforming the untransformable: application of direct transformation to manipulate genetically *Staphylococcus aureus* and *Staphylococcus epidermidis*. *Mbio* 3(2).
4. Chen J, Yoong P, Ram G, Torres VJ, & Novick RP (2014) Single-copy vectors for integration at the SaPI1 attachment site for *Staphylococcus aureus*. *Plasmid* 76:1-7.
5. Chapman JR, *et al.* (2017) Using Quantitative Spectrometry to Understand the Influence of Genetics and Nutritional Perturbations On the Virulence Potential of *Staphylococcus aureus*. *Mol Cell Proteomics* 16(4 suppl 1):S15-S28.
6. Carroll RK, Weiss A, & Shaw LN (2016) RNA-Sequencing of *Staphylococcus aureus* Messenger RNA. *Methods Mol Biol* 1373:131-141.
7. Martin M (2011) Cutadapt removes adapter sequences from high-throughput sequencing reads. *EMBnet.journal* 17(1):10.
8. Langmead B & Salzberg SL (2012) Fast gapped-read alignment with Bowtie 2. *Nat Methods* 9(4):357-359.
9. Anders S, Pyl PT, & Huber W (2015) HTSeq--a Python framework to work with high-throughput sequencing data. *Bioinformatics* 31(2):166-169.
10. Ritchie ME, *et al.* (2015) limma powers differential expression analyses for RNA-sequencing and microarray studies. *Nucleic Acids Res* 43(7):e47.
11. Law CW, Chen Y, Shi W, & Smyth GK (2014) voom: Precision weights unlock linear model analysis tools for RNA-seq read counts. *Genome Biol* 15(2):R29.
12. Balasubramanian D, *et al.* (2016) *Staphylococcus aureus* Coordinates Leukocidin Expression and Pathogenesis by Sensing Metabolic Fluxes via RpiRc. *Mbio* 7(3).

13. Reimand J, Kull M, Peterson H, Hansen J, & Vilo J (2007) g:Profiler--a web-based toolset for functional profiling of gene lists from large-scale experiments. *Nucleic Acids Res* 35(Web Server issue):W193-200.
14. Jones P, *et al.* (2014) InterProScan 5: genome-scale protein function classification. *Bioinformatics* 30(9):1236-1240.
15. Becker SH, *et al.* (2019) The Mycobacterium tuberculosis Pup-proteasome system regulates nitrate metabolism through an essential protein quality control pathway. *Proc Natl Acad Sci U S A* 116(8):3202-3210.
16. Eng JK, McCormack AL, & Yates JR (1994) An approach to correlate tandem mass spectral data of peptides with amino acid sequences in a protein database. *J Am Soc Mass Spectrom* 5(11):976-989.
17. Reyes-Robles T, *et al.* (2013) Staphylococcus aureus leukotoxin ED targets the chemokine receptors CXCR1 and CXCR2 to kill leukocytes and promote infection. *Cell Host Microbe* 14(4):453-459.
18. Alonzo F, 3rd, *et al.* (2012) Staphylococcus aureus leucocidin ED contributes to systemic infection by targeting neutrophils and promoting bacterial growth in vivo. *Molecular microbiology* 83(2):423-435.
19. Blake KJ, *et al.* (2018) Staphylococcus aureus produces pain through pore-forming toxins and neuronal TRPV1 that is silenced by QX-314. *Nat Commun* 9(1):37.